# 9

#### **Research Article**

Rakesh Goswami\*, Anita Khosla, Aftab Alam and Pradeep K. Varshney

# Synthesis and characterization of sustainable hybrid bio-nanocomposite of starch and polypropylene for electrical engineering applications

https://doi.org/10.1515/jmbm-2025-0038 received August 27, 2024; accepted January 08, 2025

Abstract: Plasticized potato starch being a sustainable, renewable, and cost-effective reinforcement has been melt mixed in this study with nano-TiO<sub>2</sub> and polypropylene (PP) and compression molded into test specimens. Starch concentration was kept at 20%, whereas nano-TiO<sub>2</sub> was varied as 1, 3, and 5% in the hybrid composites. Investigations were done for the dispersion of TiO<sub>2</sub> and starch in the base polymer, and studies for the impact of nano-TiO2 on the mechanical, electrical, and thermal characteristics were also done. No adversative degradation in the dry arc resistance and dielectric property of the PP composites was found even at high starch loading of 20%, whereas mechanical characterization revealed a decline in percentage elongation and flexural strength but nearly similar tensile and impact strengths. Dynamic mechanical analysis studies showed a decrease in the mechanical strength of the biocomposite PPST-20, which improved upon the fusion of nano-TiO2. Uniform dispersion of nano-TiO2 in the morphological structure was examined using scanning electron microscopy, whereas intact melting behavior and increased crystallization temperature indicating the nucleating effect of nanofiller were verified using differential scanning calorimeter

studies. Two-stage degradation patterns due to biomaterial and PP were also evident in the thermo gravimetric analysis studies.

**Keywords:** electrical properties, hybrid bio-composite, mechanical properties, nano-TiO<sub>2</sub>, polypropylene, starch

## 1 Introduction

Polypropylene (PP) and its composites are one of the most consumed and most cost-advantageous commodity polymers in the field of mechanical, electrical, and electronics engineering. PP is a non-biodegradable and petroleumbased material, which exhibits extraordinary mechanical, electrical, and thermal properties, i.e., lower density, high crystallinity, excellent elasticity, stiffness, hardness, better tensile properties, high thermal stability, resistance to fatigue, high electrical resistivity, high dielectric strength, but lower dielectric loss [1]. Inherently exceptional properties of these composites have made them one of the widely used materials for battery separators, electrical wire insulation, switches, transducers, capacitors, field emission displays, EMI shielding, control cables, thin wall applications, etc. As per the report of "ChemAnalyst," the worldwide PP market, which stood at 74 million tonnes in 2022, is projected to reach 114 million tons by 2030. Such high consumption of PP may be a catastrophic or environmental disaster if left without proper checks, balances, and disposal [2,3]. To reduce the production cost, and simultaneously enhance the electrical, mechanical, and chemical characteristics of the PP-based composite materials, fillers and nanomaterials were incorporated into it [4] by researchers. Lewis, a material scientist, highlighted that [5] "nano-fillers with a diameter of less than 100 nm usually disperse homogeneously into base polymers, thus enhancing the properties of respective polymer matrix." With the insight of this observation, Lewis brought the attention of material scientists to

Anita Khosla: Department of Electrical and Electronics Engineering, SET, Manav Rachna International Institute of Research and Studies, Faridabad, Haryana, 121004, India, e-mail: anitakhosla.set@mriu.edu.in Aftab Alam: Department of Polymer Technology, Guru Nanak Dev DSEU Rohini Campus, Sector 15, Rohini, Delhi, 110089, India, e-mail: aftab.alam@dseu.ac.in

**Pradeep K. Varshney:** Department of Academic Processes and Quality Assurance, Swami Rama Himalayan University, Jolly Grant, Dehradun, Uttarakhand, 248016, India, e-mail: varshney70@rediffmail.com

<sup>\*</sup> Corresponding author: Rakesh Goswami, Department of Electrical and Electronics Engineering, SET, Manav Rachna International Institute of Research and Studies, Faridabad, Haryana, 121004, India, e-mail: rakesh.goswami@dseu.ac.in

2 — Rakesh Goswami et al. DE GRUYTER

nano-dielectric materials and their electrical breakdown phenomena. This understanding was later extended by Tanaka in a separate study [6,7]. Another researcher, Usuk *et al.*, extended previous studies and presented the composite of PP/clay as the first-ever nano-dielectric material [8]. This research formed the basis to incorporate nanomaterials such as MgO [9], silica [10], CNT [11], and graphene [12] in the PP-based nano-dielectric materials. Despite several concurrent studies in the field of PP composite materials for electrical and electronics engineering, a significant influence of poor impact strength and Young's modulus of pure PP limits its extensive application in high voltage applications [1,13]. PP-based non-woven fabrics were also developed and investigated for application as battery separators in several other research [14–23].

The rapid pace of industrialization and concern with seeking sustainable industrial materials has necessitated the incorporation of several bio-materials in the polymeric matrix for reduced dependency on petroleum-based polymers [24-26]. Thermoplastic starch (TPS) being a renewable, sustainable, and low-cost bio-material has shown the potential to reduce the burden on fossil materials. Several researchers in the recent past have successfully blended thermoplastic starch and suitable compatibilizers with PP/PE for improved thermal and mechanical characteristics [27–30]; however, the hydrophilic nature and poor mechanical properties of starch limited its application in the electrical and electronics engineering field. Nano-TiO<sub>2</sub> is another low-cost material readily compatible with the PP matrix, which offers characteristics to offset the majority of the starch-induced property degradation in the composite material. The distinctly high dielectric constant, UV stabilization, chemical inertness, anti-bacterial property, and high refractive index of the nano-TiO<sub>2</sub> [31-35] make it a nanofiller desirable for blending with bio-composite of starch and PP. Incorporation of starch and nano-TiO2 as fillers simultaneously in the polymer matrix has some inherent difficulties, i.e., formation of agglomerate of nanoparticle, largely because of its long chain organic origin, semicrystalline nature, and its intercalation into bio-polymer. Such factors cause poor mechanical, thermal, and optical properties of bio-nanocomposites; thus, dispersion and intercalation of nanofillers pose the principal challenge in the synthesis of starch and nano-TiO2-based bionanocomposites [36-38]. This study addresses this challenge by synthesis and characterization of the hybrid composites of TPS, nano-TiO<sub>2</sub>, and PP using the thermokinetic melt mixing method. The content of the starch and compatibilizer in PP was kept at 20 and 10% separately, while the content of nano-TiO<sub>2</sub> was varied as 1, 3, and 5%, and composites were named PPSTTiO<sub>2</sub>-2001, 2003, and 2005, respectively. Hybrid bio-nanocomposites have been melt mixed using an ultrahigh-speed

thermokinetic mixer, which exerts high shear force for rapid and homogeneous melt mixing of base polymer with bio- and nanofillers. This method of composite blending allows uniform distribution of compatibilizer and filler particles in the polymeric matrix. The hybrid bio-nanocomposite obtained was evaluated for electrical, mechanical, and thermal characterizations, and the role of the starch and nano-TiO<sub>2</sub> loading was also discussed to discover the relationship between morphology and properties.

# 2 Experimental

#### 2.1 Materials

PP (homo polymer) with melt flow index (MFI) of 35 g  $10~\rm min^{-1}$  and 2.16 kg at 230°C was used as a base polymer. Thermoplastic potato starch with a molecular weight of 162.14 was used as a bio-filler. The glycerol of 99.5% purity was used as a plasticizer and maleic anhydride grafted PP (PP-g-MA) was used as a compatibilizer. The nano-TiO<sub>2</sub> of particle size 20–80 nm and rutile grade with surface area  $19.2~\rm m^2~g^{-1}$  acquired from Tata Chemicals was used as a nanofiller.

# 2.2 Preparation of PP, starch, and nano-TiO<sub>2</sub> bio-nanocomposite

Hybrid bio-nanocomposite of PP was prepared in two stages. In the first stage, the starch powder was homogeneously mixed with 25% glycerol (w/w) using a mixer and kept overnight for swelling. The next day, the suspension was melt mixed uniformly with the PP and nano-TiO<sub>2</sub> in an ultrahigh-speed thermo-kinetic mixer and the melt mix so obtained of nano-TiO2, starch, and PP was molded into ASTM standard test specimen in a compression molding machine. The formulation of the hybrid bio-nanocomposite is mentioned in Table 1.

Table 1: Formulation of bio-composite of starch, nano-TiO<sub>2</sub>, and PP

Sample name	PP (grade)	% starch	% nano-TiO <sub>2</sub>	PP-g-MA
PP	100	0	0	0
PPST-20	70	20	0	10
PPSTTiO <sub>2</sub> -2001	69	20	1	10
PPSTTiO <sub>2</sub> -2003	67	20	3	10
PPSTTiO <sub>2</sub> -2005	65	20	5	10

#### 3 Characterization

# 3.1 Fourier transmission infrared spectroscopy (FTIR)

FTIR spectrum of all five molded specimens was recorded in the IRSpirit-X series (M/s Shimadzu Corporation, Japan). The samples were analyzed in a wavelength of 400–4,000 cm<sup>-1</sup> in absorbance method.

#### 3.2 Thermal properties

#### 3.2.1 Differential scanning calorimeter (DSC)

The DSC data of the bio-composites and bio-nanocomposite specimens have been assessed in the presence of inert gas "nitrogen." Specimens were heated from -50 to 200°C at a rate of 10°C min<sup>-1</sup>, the temperature was kept constant at 200°C for 5 min, and then, specimens were cooled down at the same rate. Melting temperature " $T_{\rm m}$ ," crystallization temperature " $T_c$ ," change in energy " $\Delta H_m$ " and " $\Delta H_c$ ," and degree of crystallinity "Xc" (38) have been documented from the peaks and area under the DSC thermogram.

#### 3.2.2 Thermo gravimetric analysis (TGA)

The TGA data of the bio-composites and bio-nanocomposite specimens have been assessed in the presence of inert gas "nitrogen" to avoid oxidation. Specimens were heated from 50 to 650°C at a rate of 10°C min<sup>-1</sup>, and percentage weight loss at the different temperatures has been documented.

#### 3.3 Dynamic mechanical analysis (DMA)

The DMA data of the formulations have also been calculated in the presence of inert gas "nitrogen" to avoid oxidation. Specimens were heated from 25 to 160°C at a rate of 03°C min<sup>-1</sup>, with a strain amplitude of 0.05%. Under the varying temperature, change in the storage modulus (E') and Loss factor (tan  $\delta$ ) was measured at 1 Hz.

# 3.4 Tensile properties

For the evaluation of the tensile properties, the formulations were pre-conditioned at 23°C temperature, and relative humidity of 50% for 24 h. The test was done as per ASTM D 638 standards at 23°C and the speed of the crosshead was kept at 50 mm min<sup>-1</sup>. The average results from the five identical specimens were used as the tensile strength of respective formulations.

### 3.5 Flexural properties

For the evaluation of the flexural properties, the formulations were pre-conditioned at 23°C temperature, and relative humidity of 50% for 24 h. The test was done as per ASTM D 790 standards and the speed of the cross-head was kept at 05 mm min<sup>-1</sup>. The average results from the five identical specimens were used as the flexural values of respective formulations.

#### 3.6 Impact strength

For the evaluation of the Impact properties, the formulations were pre-conditioned at 23°C temperature and relative humidity of 50% for 40 h. The test was done as per ASTM D 256 standards and the energy of the hammer was kept at 2.75 J. The average results from the five identical specimens were used as the impact strength of respective formulations.

#### 3.7 MFI

The MFI test of the bio-nanocomposites has been done as per ASTM D 1238 standards. The test was done at 230°C under a loading condition of 2.16 kg. The average results from the five identical specimens were used as the melt value of respective formulations.

#### 3.8 Scanning electron microscopy (SEM)

SEM instrument from Hitachi-Japan, model no S-3700 N, was used to obtain the microstructure of samples. The morphological analysis was performed on fractured surfaces of compression-molded samples. The dried samples were first sputter-coated with a golden layer and scanned under a vacuum.

#### 3.9 Electrical properties

The dry arc resistance tester and high voltage breakdown tester of M/s Sensor, India, were used to estimate the electrical properties of samples as per standards ASTM D 495 for dry arc resistance and ASTM D 149 for dielectric strength. The specimen was evaluated for its ability to withstand the arcing and breakdown at high voltage when exposed to a high electric voltage of 12.5 kV s<sup>-1</sup> and 500 V s<sup>-1</sup> rate of rise.

# 4 Results and discussion

#### 4.1 FTIR spectroscopy

Figure 1 shows the FTIR image of PP and its composites with thermoplastic potato starch and different compositions of nano-TiO<sub>2</sub>.

FTIR spectroscopy was employed to verify the compatibilization between PP, thermoplastic potato starch, and nano-TiO2. Several absorbance peaks in the spectrum indicate interlinking of molecular bonds of PP, starch, and nano-TiO<sub>2</sub>. Peaks at 3,300–3,800 cm<sup>-1</sup> indicate O–H bond, peaks at 1744.3 cm<sup>-1</sup> indicate C=O bond, peaks at 1255.69 cm<sup>-1</sup> indicate -O-C(O)- and C-OH bonds, peaks at 1152.36 cm<sup>-1</sup> indicate C-O-C bond, and peaks at 1025.36 cm<sup>-1</sup> indicate C-O bond; these characteristic peaks and corresponding bond indicate the presence of thermoplastic starch [39,40]. The peak observed near 1744.3 cm<sup>-1</sup> indicates the presence of an anhydride group as the PP backbone; this also indicates the linkage between biomaterial and PP [39]. The CH<sub>3</sub> bonds at 2950.5, 2867.28, and 1376.23 cm<sup>-1</sup>, the CH<sub>2</sub> bonds at 2837.14 and 1454.4 cm<sup>-1</sup>, and three isotactic peaks at 1167.43, 997.3, and 972.9 cm<sup>-1</sup> confirmed the existence of the PP matrix in all the polymeric bio-nanocomposites. The peak at about 840.9 and 807.9 cm<sup>-1</sup>

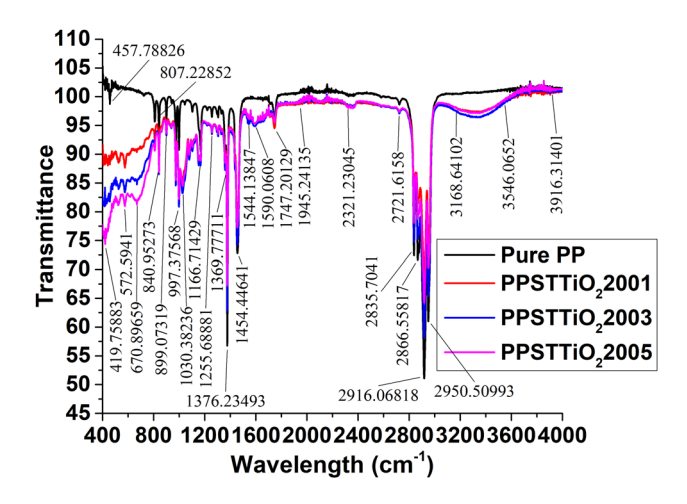


Figure 1: FTIR spectra of PP, PPSTTiO<sub>2</sub>-2001, 2003, and 2005.

is attributable to Ti–O, and another vibration at  $420 \, \mathrm{cm}^{-1}$  may be associated with a TiO–Ti vibration [41]. The stretching vibration and corresponding absorbance peak at  $800 \, \mathrm{cm}^{-1}$  may be associated with the Ti–O bond. The bonds at 760, 680, 560, 500, and  $468 \, \mathrm{cm}^{-1}$  can be linked to the TiO–Ti bond [42,43], which further confirms the presence of nano-TiO<sub>2</sub> in the bio-nanocomposites.

#### 4.2 Thermal properties

The DSC thermogram in Figure 2 indicates the thermal properties of bio-nanocomposite material. The heat flow through the nanocomposite of PP, thermoplastic starch, and nano-TiO<sub>2</sub> was studied with the view to get the transition points to the  $T_{\rm m}$ ,  $\Delta H_{\rm m}$ , and  $X_{\rm c}$ . The peaks and enthalpy observed from Figure 2 are summarized in Table 2, which indicates that the thermal properties of bio-composites remain almost intact even after loading of bio- and nanofillers.

DSC data reveal the melting temperature of the pure PP as 154.19°C, which remains nearly unaffected even after the blending of 20% thermoplastic potato starch and nano-TiO<sub>2</sub> up to 5%. The crystallization temperature of all the bionanocomposites was found to increase slightly by 6.35–7.24%; this can be attributable to the nucleating action of the welldispersed nano-TiO<sub>2</sub> [44]. The degree of crystallinity of the bio-composite, i.e., PPST-20 decreased by -19.74%, which decreased further by -23.35 and -23.46% in PPSTTiO<sub>2</sub>-2001 and PPSTTiO2-2005, respectively, but increased to a net decrease of -15.23% in PPSTTiO2-2003. An increase in the crystallinity of PPSTTiO<sub>2</sub>-2003 confirms the nucleating effect of the finely dispersed nano-TiO2. A decline in these properties in the case of PPSTTiO<sub>2</sub>-2001 and 2005 was also observed, which can be attributable to the physical hindrance because of the semi-crystalline character of starch, its long-chain organic structure, and aggregate form, when subject to heat and stress in the polymer matrix [45]. The crystallinity first reduced and then increased after the addition of 3% nano-TiO<sub>2</sub> in the bio-nanocomposites, which reduced again at 5% nano-TiO<sub>2</sub> loading. Maximum crystallinity has been observed in PPSTTiO<sub>2</sub>-2003, which declined again in PPSTTiO<sub>2</sub>-2005. Reduced crystallinity of the hybrid composite with 5% nano-TiO<sub>2</sub> can be attributable to the agglomeration of nanoparticles at higher concentrations. Bonding of the hydroxyl group of TPS with nano-TiO<sub>2</sub>, strong attraction force between the particles of nanomaterial, and insufficient diffusion at 5% nanofiller loading causes filler particles to bind together and agglomerate. Hinderance in the close packing of filler particles in the bio-nanocomposite and thermoplastic-starch-induced flexibility are also seen. Such factors seem to have been neutralized to a

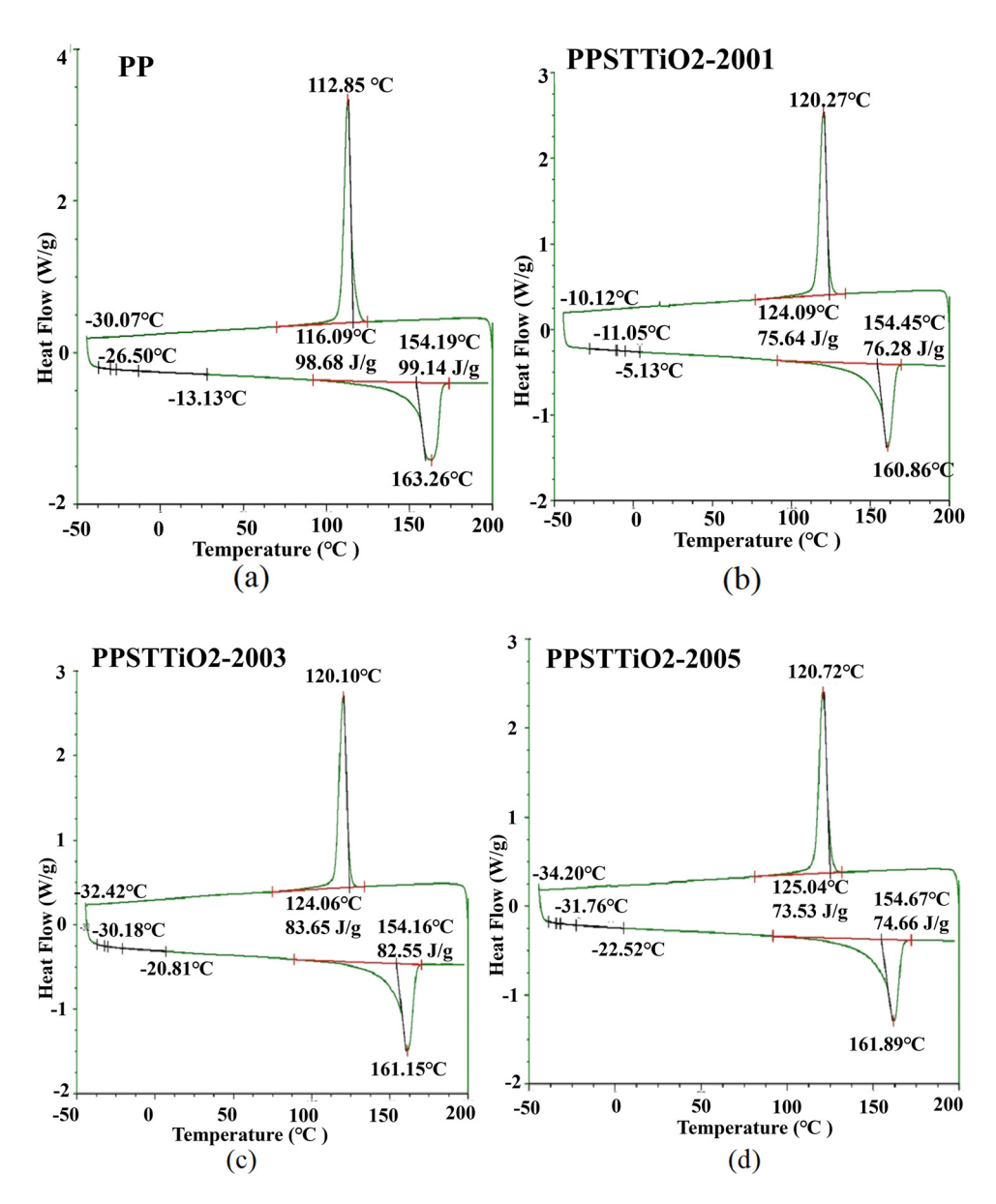


Figure 2: DSC thermogram of (a) PP, (b) PPSTTiO<sub>2</sub>-2001, (c) PPSTTiO<sub>2</sub>-2003, and (d) PPSTTiO<sub>2</sub>-2005.

Table 2: The DSC detailed data of PP, PPSTTiO<sub>2</sub>-2001, 2003, and 2005

Sample	T <sub>m</sub> (°C)	$\Delta H_{\rm m}$ (J g <sup>-1</sup> )	<i>T</i> <sub>c</sub> (°C)	Δ <i>H</i> <sub>c</sub> (J)	<i>X</i> <sub>c</sub> (%)
PP	154.19	99.14	116.68	98.68	51.94
PPST-20	154.10	76.33	125.13	79.20	41.68
PPSTTiO <sub>2</sub> -2001	154.45	76.28	124.09	75.64	39.81
PPSTTiO <sub>2</sub> -2003	154.16	82.55	124.06	83.65	44.02
PPSTTiO <sub>2</sub> -2005	154.67	74.66	125.04	75.53	39.75

great extent by the nucleating action of nano-TiO<sub>2</sub>, particles, thus increasing the thermal stability and crystallinity of the bio-nanocomposite material.

#### 4.3 TGA

Figure 3 shows the TGA thermograms of the hybrid bionanocomposite and Tables 3 and 4 present percentage mass loss at 10, 90, and 90% and at 120, 250, 350, 450, and 550°C, respectively.

Starch is a thermally less stable polymer when compared with PP and nano-TiO2. Despite this, the TGA thermogram of PPSTTiO<sub>2</sub>-2001, 2003, and 2005, when compared to that of PPST-20, shows improved thermal stability to decomposition even after the loading of 20% thermoplastic starch and nano-TiO2 up to 5% in the PP matrix. Thermal degradation of the thermoplastic starch involves 6 — Rakesh Goswami et al. DE GRUYTER

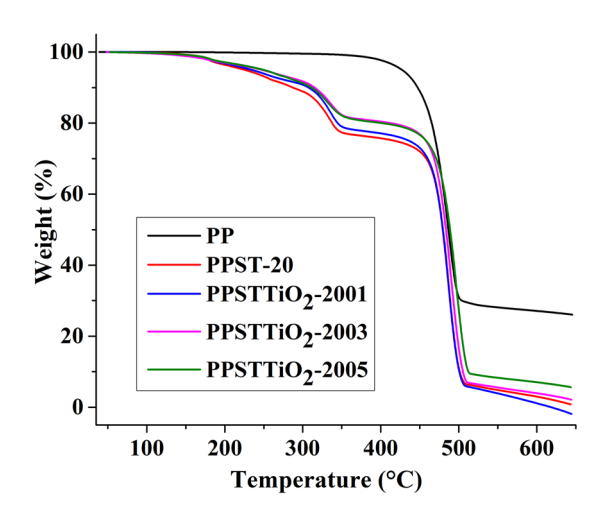


Figure 3: TGA thermogram of PP, PPSTTiO<sub>2</sub>-2001, 2003, and 2005.

Table 3: Decomposition temperature and % weight loss

Sample	T <sub>d</sub> (-10)	T <sub>d</sub> (-50)	T <sub>d</sub> (-90)
PP	446.97	486.32	_
PPST-20	287.09	479.23	500.89
PPSTTiO <sub>2</sub> -2001	307.41	479.48	500.43
PPSTTiO <sub>2</sub> -2003	315.11	483.45	505.04
PPSTTiO <sub>2</sub> -2005	311.17	488.45	512.10

dehydration, ring scission, and decomposition. TGA studies, in confirmation of the degradation behavior of starch, showed a significant increase in the thermal degradation of starch-based bio-composite PPST-20, which improved significantly upon the addition of nano-TiO $_2$ . Comparative TGA thermogram with and without starch/nano-TiO $_2$  shows the highest decomposition rate and 10% decomposition at 287°C in the case of bio-composite with 20% starch. This improved significantly to 307, 315.17, and 311.17°C in the case of 1, 3, and 5% nano-TiO $_2$  loading, respectively. The second stage of degradation of PPST-20 above 550°C was attributed to the

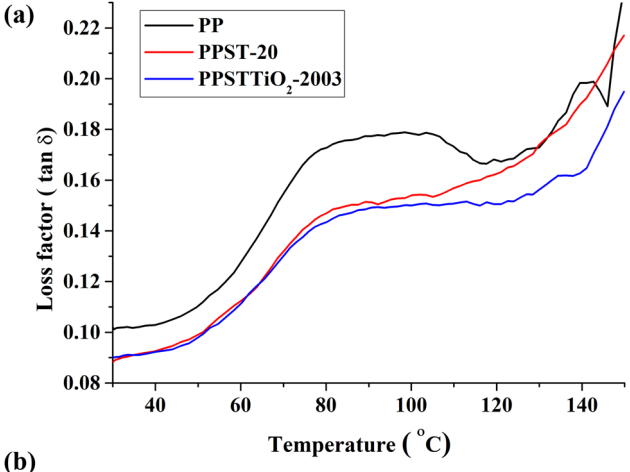
**Table 4:** Effect of thermoplastic starch and nano-TiO<sub>2</sub> on thermal degradation of PP and hybrid bio-nanocomposite

Sample	I (120°C)	I (250°C)	I (350°C)	I (450°C)	I (550°C)
PP	0	0.25	0.77	11.05	28
PPST-20	0.26	6.83	22.62	28.01	95.15
PPSTTiO <sub>2</sub> - 2001	0.32	6.05	20.97	26.97	96.12
PPSTTiO <sub>2</sub> - 2003	0.55	5.13	17.65	23.14	94.45
PPSTTiO <sub>2</sub> - 2005	0.46	5.03	17.85	23.34	91.71

breakdown of PP, which involved the breakage of C–C and C–H bonds. Among all the formulations, bio-nanocomposite with 3% nano-TiO $_2$  showed thermal decomposition at the lowest rate, thus increasing the thermal stability. TGA results therefore conform to the findings of DSC studies. Changes in the thermal properties from DSC and TGA studies both point to an effective distribution of nanoparticles in the polymer matrix, effective plasticization effect of glycerol, PP-g-MA, and nucleating action of nano-TiO $_2$  at lower concentrations of 1 and 3%.

#### **4.4 DMA**

The bio-nanocomposite of PP-based polymeric matrix is expected to exhibit some elastic response, which can be evaluated in the DMA study by investigating the change in loss factor ( $\tan \delta$ ) and storage modulus (E) represented in Figure 4(a) and (b), respectively.



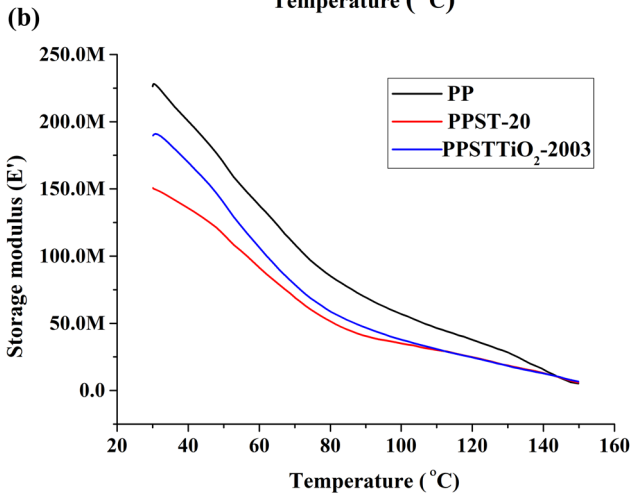


**Figure 4:** (a) Loss factor (tan  $\delta$ ) of PP, PPST-20, and PPSTTiO<sub>2</sub>-2003. (b) Storage modulus of PP, PPST-20, and PPSTTiO<sub>2</sub>-2003.

DMA study in Figure 4 enables us to evaluate the damping properties, stiffness, and mechanical strength of the specimen. The plot of tan  $\delta$  against temperature as shown in Figure 4(a) shows the decline in the tan  $\delta$  value of pure PP upon the blending of starch and nano-TiO<sub>2</sub>. This graph shows lower energy dissipation, indicating a slight increase in the rigidity and brittleness of the hybrid composite material when compared with the pure PP, and the same was verified by tensile, flexural, and impact studies. The loss factor (tan  $\delta$ ) of the hybrid biocomposites PPST-20 and bio-nanocomposite PPSTTiO<sub>2</sub>-2003 remained almost the same at lower temperatures, but started improving above 70°C in PPSTTiO<sub>2</sub>-2003 and subsequently became nearly equal to that of pure PP at around 120°C. These results indicate improvement in the damping property of PPSTTiO<sub>2</sub>-2003 at a temperature exceeding 70°C. Another graphical representation shown in Figure 4(b) represents comparative stored energy in the pure PP and bio-nanomaterial. Results from this graph show a considerable decrease in the stored energy in PPST-20 at temperatures below 100°C, which improved to a great extent in the bionanocomposite PPSTTiO<sub>2</sub>-2003. The decrease in stored energy

of PPST-20 and the subsequent increase in PPSTTiO<sub>2</sub>-2003 imply a significant increase in the flexibility of bio-composite, which is reduced to a great extent in PPSTTiO<sub>2</sub>-2003 but remains greater than pure PP. The PP-g-MA in the bio-nanocomposite material and the plasticization effect of thermoplastic starch seem to have induced changes in the DMA properties of PPST-20 and PPSTTiO<sub>2</sub>-2003. These changes can also be attributable to the increased interfacial compatibility between pure PP and fillers, *i.e.*, starch and nano-TiO<sub>2</sub>. DMA results in this regard are also supported by results derived from the thermal studies and SEM studies.

#### 4.5 Mechanical properties

Figure 5 shows the mechanical properties of the bio-nano-composite formulations under investigation.

The tensile strength, % elongation, impact strength, and flexural strength of PPST-20, PPSTTiO<sub>2</sub>-2001, 2003, and 2005 were compared with each other and to that of pure PP in Figure 5. Results show an obvious decline in all the

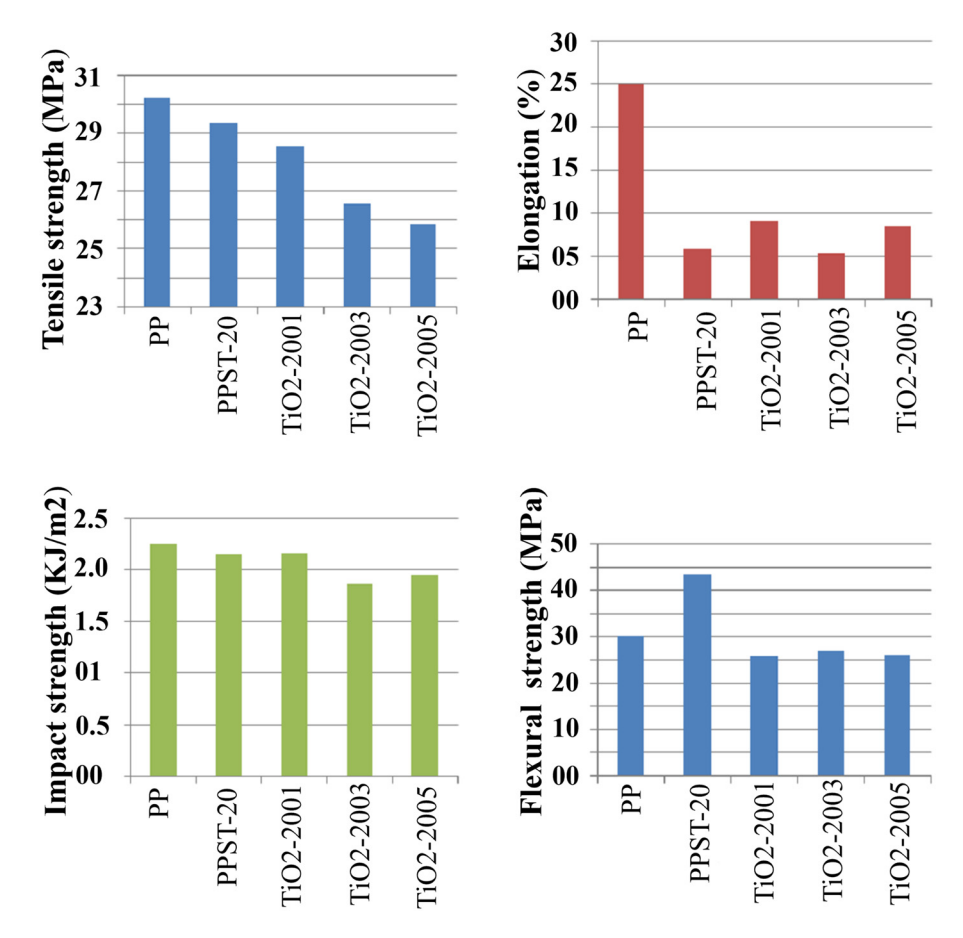


Figure 5: Mechanical properties of the PP, PPST-20, and PPSTTiO<sub>2</sub>-2001, 2003, and 2005.

mechanical properties of biocomposites and bio-nanocomposite material upon blending starch and nano-TiO<sub>2</sub>. Such deterioration in properties can mainly be attributable to the function of starch and nano-TiO2 as particulate filler in PP-based composite materials; this result is confirmed by the change in flexural strength of PPST-20. It is apparent from Figure 5 that the bio-nanocomposite shows the impact strength to be nearly comparable to the pure PP and PPST-20, as verified by the findings of the DMA studies. The blending of TPS enhanced the flexural strength of the blend, but the addition of nano-TiO2 reduced it by 30%, which can be attributable to the weak union of nano-TiO<sub>2</sub> with the PP matrix. As far as change in the tensile and elongation properties of the bionanocomposite is concerned, a substantial decline in the tensile strength was observed in all the specimens; however, % elongation was found more than that of PPST-20 but considerably less than that of pure PP. Such wide variation of the mechanical properties confirms the weak bonding of starch molecules with the PP matrix, which improved substantially because of the nucleating action of nano-TiO2 molecules.

#### 4.6 MFI

The MFI test values of different formulations, *i.e.*, PP, PPST-20, PPSTTiO<sub>2</sub>-2001, 2003, and 2005, are shown in Figure 6.

The highest MFI values of the PPST-20 among all the formulations point toward the plasticization effect of the 20% thermoplastic starch and uniform diffusion of filler particles in the polymer matrix. The presence of nano- ${\rm TiO_2}$  in the bio-nanocomposites decreases the MFI values by 50%, attributable to the surface roughness of inorganic particle fillers  ${\rm TiO_2}$  when compared with thermoplastic starch. This result validates the results from the DMA study and mechanical characterization.

#### 4.7 Morphological analysis

Figure 7 illustrates the typical SEM images of the fractural surface of pure PP and bio-nanocomposites. Image points toward starch molecules in granule form and nano-TiO<sub>2</sub> particles in particulate forms in PP, PPSTTiO2-2001, 2003, and 2005. The images also reveal that thermoplastic starch and nano-TiO<sub>2</sub> are uniformly distributed in the polymer matrix, thus forming a homogeneous phase of bio-nanocomposite.

Results also indicate the action of coupling agent PP-g-MA, which reduced the interfacial energy, thus increasing the interfacial cohesion amongst phases of the TPS, nano-TiO<sub>2</sub>, and PP matrix. SEM image exhibited nano-TiO<sub>2</sub> molecules to be strongly nested in the polymer matrix, thus improving the compatibility and cohesion among the filler particles and polymer matrix. These enhancements caused the advancement of mechanical, thermal, and morphological characteristics of the bio-nanocomposites. Such results are in validation of the comparative change in the tensile strength, % elongation, impact strength, and flexural strength of PPST-20, PPSTTiO<sub>2</sub>-2001, 2003, and 2005.

#### 4.8 Electrical properties

Table 5 represents the dry arc resistance and di-electric strength of samples under test.

During the electrical testing, bio-nanocomposite material "PPSTTiO<sub>2</sub>-2003" displays excellent dry arc resistance, which is as close as 94.3% of the pure PP, but other samples stood at a marginal low value of 88%. This result indicates localized breakdown because of thermal erosion and chemical degradation when exposed to a high voltage of 12.5 kV. As far as the electric di-electric strength of the specimen under test, all the developed hybrid bio-composite materials

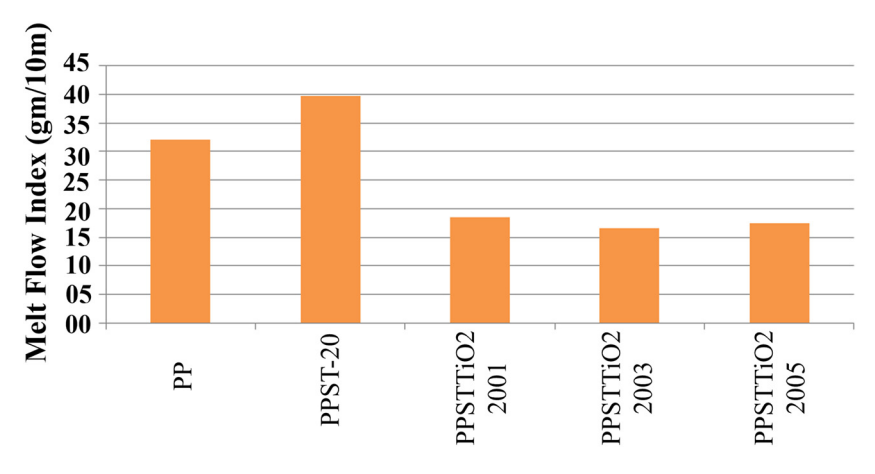


Figure 6: MFI of PP, PPST-20, and PPSTTiO<sub>2</sub>-2001, 2003, and 2005.

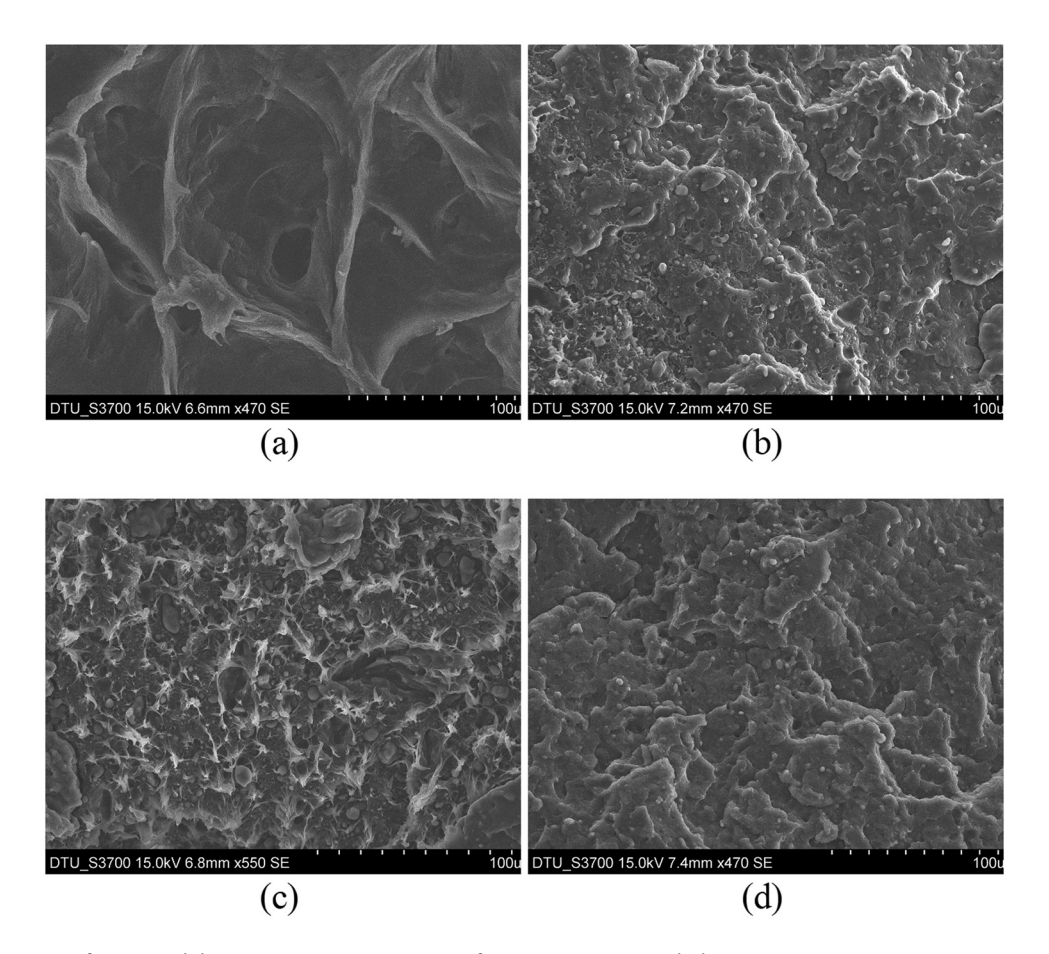


Figure 7: SEM image of (a) PP and (b) PPSTTiO<sub>2</sub>-2001. SEM image of (c) PPSTTiO<sub>2</sub>-2003 and (d) PPSTTiO<sub>2</sub>-2005.

display slightly improved dielectric strength between 10 and 12 kV against 10 kV of the pure polymer. Despite the polar nature of starch molecules, the dielectric environment within the PP matrix appears to be largely unchanged because of the uniform distribution of starch molecules and the nucleating action of nano-TiO<sub>2</sub>. Such phenomena cause improved electrical properties of the bio-nanocomposite.

# 5 Conclusion

This research work employs a thermo-kinetic melt mixing method for the synthesis of sustainable composite material

of pure PP, potato starch, and nano-TiO<sub>2</sub> and retains the excellent mechanical, thermal, and electrical properties of PP as far as possible. Synthesis involves the blending of pure PP as base polymer, 20% potato starch as bio filler (in PPST-20), nano-TiO<sub>2</sub> as nanofiller (1, 3, and 5% in PPSTTiO<sub>2</sub>-2001, 2003, and 2005, respectively), and maleic anhydride grafted polypropylene (PP-g-MA) as compatibilizer. The morphological characterization based on the SEM image shows a uniform distribution of the thermoplastic starch and nano-TiO<sub>2</sub> particles in the polymer matrix. This indicates the action of PP/PP-g-MA in increasing the scattering of nano-TiO<sub>2</sub> and starch particles in the polymer matrix. The SEM images of nano-TiO<sub>2</sub> nanocomposite were found to be quite stable and

Table 5: Electrical characteristics of bio-composite

Sample	Dry arc resistance test at 12.5 kV, ASTM D 495 (s)	Di-electric strength ASTM D 149 (kV)
PP	193	11
PPST-20	170	12
PPSTTiO <sub>2</sub> -2001	170	10
PPSTTiO <sub>2</sub> -2003	182	11
PPSTTiO <sub>2</sub> -2005	170	12

nano-TiO<sub>2</sub> particles were found well embedded in the polymeric matrix with thermoplastic starch. The DMA, MFI, DSC, and TGA studies also point toward strong interaction between the filler-matrix inter-phase because of the presence of maleic anhydride-based compatibilizer (PP-g-MA). Results of the DSC and TGA study indicate the action of PP-g-MA as an effective dispersing agent, consequent dispersion of all the fillers within the PP matrix, and function of nano-TiO2 as a nucleating center at lower concentrations of 1 and 3%. Thus, less thermal degradation was observed in PPSTTiO<sub>2</sub>-2001, 2003, and 2005 compared to PPST-20. The decline in the % crystallinity of all the bio-nanocomposites has also been seen. which points toward the disorder in close packing of the PP matrix. This disorder can be attributable to thermoplastic starch molecules in the polymer matrix. All the nanocomposites confirm similar thermal degradation behavior in the TGA results, but bio-nanocomposite with nano-TiO2 loading of 3 and 5% exhibits much higher thermal stability when compared to PPST-20.

The mechanical characterization has shown an increase in the flexural strength but nearly constant impact strength of PPST-20 compared to that of the base polymer. Both these properties declined further upon the addition of nano-TiO2 but remained very near to that of pure PP. The tensile strength of the PPST-20 and the other three bio-nanocomposites have also been decreasing gradually with increasing filler concentration. MFI and % elongation of the PPST-20 also reduced significantly compared to pure PP, which increased considerably with increasing nano-TiO2 concentration in the bio-nanocomposite. DMA studies also indicate a thermoplastic starch-induced decline in the loss factor (tan  $\delta$ ), signifying lower damping properties (i.e., lower energy dissipation) and a significant increase in the flexibility (i.e., storage modulus) of the PPST-20 when compared to pure PP and PPSTTiO<sub>2</sub>-2003. These DMA properties improved significantly at higher temperatures in PPSTTiO<sub>2</sub>-2003. Results of the mechanical characterization and DMA studies indicated the nucleating action of well-dispersed nano-TiO<sub>2</sub> particles in the starch-loaded PP matrix. Close packing of the bio-nanocomposite material, nucleating behavior of nano-TiO<sub>2</sub>, and increase in the matrix-filler interfacial compatibility have induced excellent electric dielectric strength and marginal decrease in arc resistance of bio-nanocomposite material. Finally, we can conclude by summarizing that the futuristic bio-nanocomposite presented in this research may reduce the reliance on fossil fuels and prove a milestone for several electrical engineering applications such as electrical insulation, dielectric material, and battery separators.

Acknowledgments: FTIR spectroscopy for the constituent polymer identification was done at University Instrumentation Centre (UIC), Manav Rachna University, Faridabad, Haryana, 121004, India. Morphological and electrical testing took place at the Department of Applied Chemistry ... Polymer Technology, Delhi Technological University, Bawana Road, Shahbad Daulatpur Village, Rohini, New Delhi, 110042, India. All tests were performed in accordance with the relevant ISO and ASTM standards.

Funding information: Authors state no funding involved.

**Author contributions:** All authors have accepted responsibility for the entire content of this manuscript and consented to its submission to the journal, they all have reviewed all the results and approved the final version of the manuscript. All the authors jointly designed the experiments. Rakesh Goswami and Aftab Alam performed the experimentation and interpretation of experimental data. Rakesh Goswami prepared the manuscript with contributions from all the co-authors.

Conflict of interest: Authors state no conflict of interest.

**Data availability statement:** All data generated or analysed during this study are included in this published article.

#### References

- [1] Dabbak SZA, Illias HA, Ang BC, Latiff NAA, Makmud MZH. Electrical properties of polyethylene/polypropylene compounds for highvoltage insulation. Energies. 2018;11(6):1448. doi: 10.3390/ en11061448.
- [2] Pearce EM. Environmentally degradable plastics. In Kirk-Othmer Encyclopaedia of chemical technology. Vol. I, 3rd edn. Hoboken, New Jersey, USA: Wiley online library, John Wiley & Sons Inc.; 1981. p. 638–68. doi: 10.1002/pol.1978.130160508.
- [3] Nair LS, Laurencin CT. Biodegradable polymers as biomaterials. Prog Polym Sci. 2007;32(8–9):762–98. doi: 10.1016/j.progpolymsci. 2007.05.017.
- [4] Pandey JC, Singh M. Dielectric polymer nanocomposites: Past advances and future prospects in electrical insulation perspective. SPE Polym. 2021;2(4):236–56. doi: 10.1002/pls2.10059.
- [5] Lewis TJ. Nanometric dielectrics. IEEE Trans Dielectr Insulation. 1994;1(5):812–25. doi: 10.1109/94.326653.
- [6] Tanaka T, Montanari GC, Mulhaupt R. Polymer nanocomposites as dielectrics and electrical insulation-perspectives for processing technologies material characterization and future applications. IEEE Trans Dielectr Insulation. 2004;11(5):763–84. doi: 10.1109/TDEI. 2004.1349782.

- [7] Tanaka T. Dielectric Nanocomposites with Insulating Properties. IEEE Trans Dielectr Insulation. 2005;12(5):914-28. doi: 10.1109/TDEI. 2005.1522186.
- [8] Usuki A, Kato M, Okada A, Kurauchi T. Synthesis of polypropyleneclay hybrid. J Appl Polym Sci. 1998;63(1):137-8. doi: 10.1002/(SICI) 1097-4628(19970103)63:1%3C137::AID-APP15%3E3.0.CO;2-2.
- Cao W, Li Z, Sheng G, Jiang X. Insulating property of polypropylene nanocomposites filled with nano-MgO of different concentration. IEEE Trans Dielectr Electr Insul. 2017;24(3):1430-7. doi: 10.1109/ TDEI.2017.006015.
- [10] Takala M, Ranta H, Nevalainen P, Pakonen P, Pelto J, Karttunen M, et al. Dielectric properties and partial discharge endurance of polypropylene-silica nanocomposite. IEEE Trans Dielectr Electr Insul. 2010:17(4):1259-67. doi: 10.1109/TDEI.2010.5539698.
- [11] Monti M, Zaccone M, Frache A, Torre L, Armentano I. Dielectric spectroscopy of PP/MWCNT nanocomposites: Relationship with crystalline structure and injection molding condition. Nanomaterials. 2021;11(2):550. doi: 10.3390/nano11020550.
- [12] Kavinkumara T, Sastikumar D, Manivannan S. Effect of functional groups on dielectric, optical gas sensing properties of graphene oxide and reduced graphene oxide at room temperature. RSC Adv. 2015;5(14):10816-25. doi: 10.1039/C4RA12766H.
- [13] Wacharawichanant S, Siripattanasak T. Mechanical and morphological properties of polypropylene/polyoxymethylene blends. Adv Chem Eng Sci. 2013;3:202-5. doi: 10.4236/aces.2013.
- [14] Yu L, Miao J, Jin Y, Lin JYS. A comparative study on polypropylene separators coated with different inorganic materials for lithium-ion batteries. Front Chem Sci Eng. 2017;11:346-52. doi: 10.1007/s11705-017-1648-9.
- [15] Feng G, Li Z, Mi L, Zheng J, Feng X, Chen W. Polypropylene/ hydrophobic-silica-aerogel-composite separator induced enhanced safety and low polarization for lithium-ion batteries. J Power Sources. 2018;376:177-83. doi: 10.1016/j.jpowsour.2017. 11.086.
- [16] Zhu W, Zhang Z, Wei J, Jing Y, Guo W, Xie Z, et al. A synergistic modification of polypropylene separator toward stable lithiumsulfur battery. J Membr Sci. 2020;597:117646. doi: 10.1016/j.memsci. 2019.117646.
- [17] Yan Y, Kong QR, Suna CC, Yuan JJ, Huang Z, Fang LF, et al. Copolymer-assisted polypropylene separator for fast and uniform lithium-ion transport in lithium-ion batteries. Chin J Polym Sci. 2020;38:1313-24. doi: 10.1007/s10118-020-2455-1.
- [18] Liu H, Yang F, Xiang M, Cao Y, Wu T. Development of multilayer polypropylene separators for lithium-ion batteries via an industrial process. Ind Eng Chem Res. 2021;60(30):11611-20. doi: 10.1021/acs. iecr.1c01577.
- [19] Moghim MH, Nahvibayani A, Eqra R. Mechanical properties of heat-treated polypropylene separators for Lithium-ion batteries. Polym Eng Sci. 2022;62(9):3049-58. doi: 10.1002/pen.
- [20] Hou J, Han L, Sun S, Li M, Yue J, Yang Y, et al. Single-walled carbon nanotubes film supported lithiated PIM-1 ultrathin selective barrier: A multifunctional layer for polypropylene separator to boost performance of Li-S batteries. Polymers. 2023;281:126137. doi: 10. 1016/j.polymer.2023.126137.
- [21] Wu Z, He X, Zhou J, Yang X, Sun L, Li H, et al. Scalable fabrication of Ni(OH)<sub>2</sub>/carbon/polypropylene separators for high-performance Li-S batteries. J Alloy Compd. 2023;935(1):168136. doi: 10.1016/j. jallcom.2022.168136.

- [22] Rahmani M, Moghim MH, Zebarjad SM, Egra H. Surface modification of a polypropylene separator by an electrospun coating layer of Poly(vinyl alchohol)-SiO for lithium-ion batteries. J Polym Res. 2023;30:129. doi: 10.1007/s10965-023-03491-2.
- Jiang Y, Sun C, Dong F, Xie H, Sun L. Multilayer polyethylene separator with enhanced thermal properties for safe lithium-ion batteries. Particuology. 2024;91:29-37. doi: 10.1016/j.partic.2023.
- [24] Rangappa SM, Puttegowda M, Parameswaranpillai J, Siengchin S, Gorbatyuk S. Advances in bio-based fiber: Moving towards a green society. Cambridge, United Kingdom: Woodhead Publishing; 2022. p. 159-91. doi: 10.1016/C2020-0-01155-2.
- [25] Doddashamachar M, Setty RNV, Reddy MVH, Johns J. Dielectric properties of banana fiber filled polypropylene composites: Effect of coupling agent. Fibers Polym. 2022;23(5):1387-95. doi: 10.1007/ s12221-022-4395-6.
- [26] Fares O, AL-Oqla F, Hayajneh M. Revealing the intrinsic dielectric properties of mediterranean green fiber composites for sustainable functional products. | Ind Text. 2022;51(5S):7732S-54S. doi: 10. 1177/15280837221094648.
- Harding KG, Dennis JS, Blottnitz HV, Harison STL. Environmental [27] analysis of plastic production processes: Comparing petroleumbased polypropylene and polyethylene with biologically-based poly-β-hydroxybutyric acid using life cycle analysis. J Biotechnol. 2007;130(1):57-66. doi: 10.1016/j.jbiotec.2007.02.012.
- Mohanty AK, Misra M, Drzal LT. Sustainable bio-composites from renewable resources: Opportunities and challenges in the green material world. J Polym Environ. 2002;10:19-26. doi: 10.1023/A% 3A1021013921916.
- [29] Griffin GJL. Starch polymer blends. Polym Degrad Stab. 1994;45(2):241-7. doi: 10.1016/0141-3910(94)90141-4.
- [30] Wu CS, Liao HT. Influence of a compatibilizer on the properties of Polethylene-Octene Elastomer/Starch Blends. J Appl Polym Sci. 2002;86(7):1792-8. doi: 10.1002/app.11199.
- [31] Harzallah OA, Dupuis D. Rheological properties of suspensions of TiO<sub>2</sub> particles in polymer solutions. 1. Shear viscosity. Rheol Acta. 2003;42:10-9. doi: 10.1007/s00397-002-0250-2.
- [32] Lange S, Arroval T, Saar R, Kink I, Aarik J, Krumme A. Oxygen barrier properties of Al<sub>2</sub>O<sub>3</sub> and TiO<sub>2</sub> coated LDPE films. Polym Plastic Technol Engg. 2015;54:301-4. doi: 10.1080/03602559.2014. 977426.
- [33] Chung YL, Ansari S, Estevez L, Hayrapetyan S, Giannelis EP, Lai HM. Preparation and properties of biodegradable starch-clay nanocomposites. Carbohydr Polym. 2010;79(2):391-6. doi: 10.1016/j. carbpol.2009.08.021.
- [34] Zhao R, Torley P, Halley PJ. Emerging biodegradable materials: Starch and protein-based bio-nanocomposite. J Mater Sci. 2008;43(9):3058-71. doi: 10.1007/s10853-007-2434-8.
- Moghaddam HM, Khoshtaghaza MH, Salimi A, Barzegar M. The TiO<sub>2</sub>-Clay-LDPE nanocomposite packaging film: Investigation on the structure and physio-mechanical properties. Polym Plastic Technol Engg. 2014;53(17):1759-67. doi: 10.1080/03602559.2014. 919647.
- [36] Youssef AM. Polymer nanocomposites as a new trend for packaging applications. Polymer-Plastic Technol Eng. 2013;52(7):635-60. doi: 10.1080/03602559.2012.762673.
- [37] Tang X, Alavi S, Herald TJ. Effect of plasticizers on the structure and properties of starch-clay nanocomposites films. Carbohydr Polym. 2008;74(3):552-8. doi: 10.1016/j.carbpol.2008.04.022.

- [38] Roy SB, Ramraj B, Shit SC, Nayak SK. Polypropylene and potato Starch Biocomposite: Phsicomechanical and Thermal Properties. J Appl Polym Sci. 2011;120(5):3078–86. doi: 10.1002/app.33486.
- [39] Gupta AP, Kumar V, Sharma M. Formulation and characterization of Biodegradable Packaging film derived from potato starch and LDPE grafted with maleic anhydride-LDPE composition. J Polym Env. 2010;18(4):484–91. doi: 10.1007/s10924-010-0213-0.
- [40] Shujun W, Jiugao Y, Jinglin Y. Preparation and characterization of compatible and degradable thermoplastic starch/polyethylene film. J Polym Env. 2006;14(1):65–70. doi: 10.1007/s10924-005-8708-9.
- [41] Devasahayam S, Sahajwalla V, Sng M. Investigation into failure in mining wire ropes – Effect of crystallinity. Open J Org Polym Mater. 2013;3(2):34–40. doi: 10.4236/ojopm.2013.32006.
- [42] Djaoued Y, Badilescu S, Ashrit PV, Robichaud J. Vibrational properties of the sol-gel prepared nanocrystalline TiO<sub>2</sub> thin films.

  Internet J Vib Spectrosc. 2001;5(6). https://www.irdg.org/ijvs/ijvs-volume-5-edition-6/vibrational-properties-of-the-sol-gel-prepared-nanocrystalline-tio2-thin-films.
- [43] Phillippi CM, Lyon SR. Longitudinal-optical phonons in TiO<sub>2</sub> (Rutile) thin-film spectra. Phys Rev B. 1971;3(6):2086–7. doi: 10.1103/ PhysRevB.3.2086.
- [44] Wang Z, Wang X, Xie G, Li G, Zhang Z. Preparation and characterization of polyethylene/TiO<sub>2</sub> nanocomposite. Compos Interfaces. 2006;13(7):623–32. doi: 10.1163/156855406778440730.
- [45] Tang X, Alavi S. Recent advances in starch, polyvinyl alcohol based polymer blends, nanocomposites and their biodegradability. Carbohydr Polym. 2011;85(1):7–16. doi: 10.1016/j.carbpol.2011.01.030.